BIRKHÄUSER

Tsunami Science
Four Years after the **2004 Indian Ocean Tsunami**

Part I: Modelling and Hazard Assessment

Edited by
Phil R. Cummins
Laura S. L. Kong
Kenji Satake

Birkhäuser
Basel · Boston · Berlin

Reprint from Pure and Applied Geophysics
(PAGEOPH), Volume 165 (2008) No. 11/12

Phil R. Cummins
Geoscience Australia
P.O. Box 378
Canberra, ACT 2601
Australia
Email: phil.cummins@ga.gov.au

Kenji Satake
Earthquake Research Institute
University of Tokyo
1-1-1 Yayoi
Bunkyo-ku
Tokyo 113-0032
Japan
Email: satake@eri.u-tokyo.ac.jp

Laura S. L. Kong
UNESCO Intergovernmental Oceanographic
Commission (IOC)
International Tsunami Information Centre
737 Bishop Street
Suite 2200
Honolulu, HI, 96813
USA
Email: l.kong@unesco.org

Library of Congress Control Number: 2009920437

Bibliographic information published by Die Deutsche Bibliothek:
Die Deutsche Bibliothek lists this publication in the Deutsche Nationalbibliografie; detailed bibliographic data is available in the Internet at <http://dnb.ddb.de>

ISBN 978-3-0346-0056-9 Birkhäuser Verlag AG, Basel · Boston · Berlin

Printed on acid-free paper produced from chlorine-free pulp. TCF ∞
Cover graphic: Based on a picture provided by Dr. Pål Wessel, Department of Geology and Geophysics, School of Ocean and Earth Science and Technology (SOEST), University of Hawaii at Manoa, Honolulu, USA.
Printed in Germany

ISBN 978-3-0346-0056-9 e-ISBN 978-3-0346-0057-6

9 8 7 6 5 4 3 2 1 www.birkhauser.ch

Contents

Pure appl. geophys. 165 (2008) 1983–1989
0033–4553/08/111983–7
DOI 10.1007/s00024-008-0423-8

Pure and Applied Geophysics

Introduction to "Tsunami Science Four Years After the 2004 Indian Ocean Tsunami, Part I: Modelling and Hazard Assessment"

PHIL R. CUMMINS,[1] LAURA S. L. KONG,[2] and KENJI SATAKE[3]

Abstract—In this introduction we briefly summarize the 14 contributions to Part I of this special issue on Tsunami Science Four Years after the 2004 Indian Ocean Tsunami. These papers are representative of the new tsunami science being conducted since the occurrence of that tragic event. Most of these were presented at the session: Tsunami Generation and Hazard, of the International Union of Geodesy and Geophysics XXIV General Assembly held at Perugia, Italy, in July of 2007. That session included over one hundred presentations on a wide range of topics in tsunami research. The papers grouped into Part I, and introduced here, cover topics directly related to tsunami mitigation such as numerical modelling, hazard assessment and databases. Part II of this special issue, Observations and Data Analysis, will be published in a subsequent volume of Pure and Applied Geophysics.

Key words: Tsunami, seiche, harbor resonance, numerical modeling, hazard assessment, inundation, tsunami mitigation, tsunami warning system, runup, tsunami database, rissaga.

1. Introduction

Four years after the 2004 Indian Ocean Tsunami, the most lethal tsunami disaster in human history, tsunami science continued to move forward rapidly. The research and disaster management community that supports tsunami mitigation has expanded greatly. Observation platforms, especially in the Indian Ocean, have far surpassed their pre-2004 capacity for detecting and measuring tsunamis and the earthquakes that most frequently cause them. A remarkable crosssection of this research was presented in the session Tsunami Generation and Hazard, at the International Union of Geodesy and Geophysics (IUGG) XXIV General Assembly in Perugia, Italy, held in July of 2007. Over one hundred presentations were made at this session, spanning topics ranging from paleotsunami research, to nonlinear shallow-water theory, to tsunami hazard and risk

[1] Geoscience Australia, GPO, Box 378, Canberra, ACT 2601, Australia.
E-mail: Phil.Cummins@ga.gov.au
[2] UNESCO IOC International Tsunami Information Centre, 737 Bishop St. Ste. 2200, Honolulu, Hawaii 96813, USA. E-mail: l.kong@unesco.org
[3] Earthquake Research Institute, University of Tokyo, 1-1-1 Yayoi, Bunkyo-ku, Tokyo 113-0032, Japan.
E-mail: satake@eri.u-tokyo.ac.jp

assessment. The IUGG's Tsunami Commission arranged for a selection of this work, along with other papers on similar topics, to be published in detail in the 28 papers of this 2-part special issue of Pure and Applied Geophysics.

In this introductory paper, we briefly discuss the papers in Part I of "Tsunami Science Four Years After the 2004 Indian Ocean Tsunami". In Section 2 we discuss new advances in the fundamental numerical techniques used to model tsunamis and Section 3 reviews several contributions that apply such techniques to improve our understanding of how near-coast processes affect tsunami propagation. Sections 4 and 5 discuss the application of tsunami modeling to tsunami hazard assessment, in a deterministic and a probabilistic sense, respectively. Section 6 describes two database efforts that are supporting researchers and warning system operators to access the most current and accurate information on tsunami events.

2. *Advances in Analytical and Numerical Modeling of Tsunamis*

The increased focus on tsunami science since the 2004 Sumatra-Andaman Earthquake and subsequent Indian Ocean Tsunami has seen a rapid expansion in the tsunami modeling community. Prior to 2004, this community consisted of a handful of research groups that utilized a few well-tested codes for numerical modeling of tsunamis. Since 2004, many more research groups have taken an interest in tsunami modeling, and these groups have in some cases either developed new codes for tsunami modeling, or adapted hydrodynamic codes that had originally been developed for other purposes. Tsunami forecasting via numerical modeling is also seeing increased use as an operational part of tsunami warning systems.

In response to this recent proliferation of tsunami modeling codes, SYNOLAKIS *et al.* (2008) pointed out the importance of validation and verification of codes used in tsunami hazard assessment or forecasting systems. They reviewed several methods by which this can be accomplished. These included analytical and laboratory validation benchmarks, as well as examples of field observations against which numerical models can be verified. A summary of the theoretical development for formulae used as analytical benchmarks was given, and details of the laboratory experiments and field observations were reviewed. In addition to the use of these benchmarks for inundation modeling in tsunami hazard studies, operational requirements for forecasting tsunamis in real-time were discussed.

ZHANG and BATISTA (2008) presented an example of the adaptation of a multi-purpose baroclinic circulation model (SELFE) to tsunami inundation and propagation. The model has several interesting features that make it a useful addition to the suite of tools already available: Release as open source, facilitating further development by a community of users; use of an unstructured grid, allowing for variable resolution to accommodate complex geometry only where necessary; an implicit time-stepping algorithm that avoids the stringent Courant–Friedrichs–Lewy stability condition, and a simple wetting/drying

algorithm that implements inundation. Along the lines suggested by SYNOLAKIS *et al.* (2008), the authors presented validation results against scenarios from the 3rd International Workshop in Long-Wave Runup Models (http://www.cee.cornell.edu/longwave).

GREENSLADE and TITOV (2008), on the other hand, use a tried and tested tsunami code (MOST – see TITOV and GOZAREZ, 1997) to compare two tsunami forecasting systems used by the U.S. National Oceanic and Atmospheric Administration (NOAA), and the Australian Bureau of Meteorology. The tsunamis caused by the 2006 Tonga and 2007 Sumatra earthquakes were used as test cases. Both systems use results of tsunami computations made prior to earthquakes and stored in a database. While the specifications of numerical simulation of tsunami propagation are very similar, the scenario sources distributed around the Pacific Basins are slightly different. The Australian system assumes different faults depending on the earthquake magnitude, while the U.S. system scales the slip amount by assimilation of tsunameter (a.k.a. DART) data. Because different sources are used to approximate the Tonga and Sumatra earthquakes, the forecasted waveforms at offshore tsunameter locations are slightly different. However, the differences in waveforms computed at coastal tide gauges are considerably smaller, indicating insensitivity of coastal tsunamis to the details of the tsunami source.

Despite substantial recent progress in numerical tsunami modeling, the rapid forecast of runup values remains a difficult problem, due to its nonlinearity and sensitivity to input data such as bathymetry and initial waveform. The paper by DIDENKULOVA *et al.* (2008) demonstrated that analytical results still have an important role to play in estimating runup. They discussed results from nonlinear shallow-water wave theory for runup of solitary tsunami waves, and showed that appropriate definitions of significant wave height and length (based on 2/3 of maximum wave height) result in formulae for computing runup characteristics that are relatively independent of incident wave shape (for symmetric incident waves). Such formulae may be used in rapidly estimating potential inundation once the tsunami height, wavelength and period in the open ocean are known.

3. Modeling of Near-Coast Effects on Tsunami Propagation

One of the most challenging aspects of tsunami modeling is accurate representation of propagation effects near the coast, including reflection and refraction by shallow bathymetry, and resonances in semi-enclosed bays and inlets. Several papers in this issue address these topics.

BABA *et al.* (2008) examined the effects of Great Barrier Reef, the world's largest coral reef located offshore Australia, on the tsunami generated by the April 1, 2007 Solomon Islands earthquake. They carried out tsunami numerical simulation from a source model based on their seismic waveform inversion. The simulated waveforms show good agreement with tide gauge data in northeast Australia. In order to examine the effect of the coral reef, they also made tsunami simulations with artificial bathymetry data

without the coral reef; the reef was replaced with deep ocean in one dataset and shallow ocean in the other. Simulations with these models indicate that the tsunami energy was reduced by direct reflection outside the reef and by refraction when the tsunami passed through the reef. As a result, the tsunami was delayed by 10–15 minutes, the amplitude became about a half or less, and the period became longer.

Semi-enclosed bays and inlets present another challenge to tsunami modeling in the form of potential resonant enhancement of tsunamis. Alberni inlet is a long ($\sim$40 km) and narrow (1–2 km) fjord in Vancouver Island, Canada. The tsunami caused by the 1964 Alaskan earthquake had a height of about 8 m above mean sea level at Port Alberni, located at the head of the inlet and about 65 km from the Pacific Ocean. FINE *et al.* (2008) examined resonance characteristics of the Alberni inlet by using numerical calculations. Their results indicated that strong amplification occurred at a period of 112 min with an amplification factor of more than 10.

VILIBIĆ *et al.* (2008) presented a comprehensive analysis of a destructive meteotsunami (*rissaga)* that occurred in the Balearic Islands in 2006. This event was not associated with an earthquake source and excited destructive harbor oscillations of several meters amplitude, resulting in an economic loss estimated at tens of millions of euros. VILIBIĆ *et al.* used a numerical model, verified using a series of measurements made during smaller *rissaga* events in 1997, and microbarograph measurement to show how the 2006 *rissaga* resulted from ocean-atmosphere resonance excited by a travelling atmospheric disturbance, which in turn induced the hazardous harbor oscillations observed. The potential for developing a *rissaga* warning system based on this model was also discussed.

4. Scenario Modeling for Tsunami Hazard Assessment

In addition to rapid tsunami forecasts that may form part of a tsunami warning, emergency managers and planners in coastal communities need information about how large tsunamis affecting their communities might be. Such questions can be answered by scenario modeling, which forms the basis of a deterministic hazard assessment. Such assessments are normally designed to encompass the worst credible, as well as the most likely, scenarios.

TIBERTI *et al.* (2008) numerically modeled potential tsunamis in the Adriatic Sea. Maximum credible earthquakes were assumed along the six source zones. They classified the computed maximum tsunami heights into three levels: marine, land and severe land for 0.05 m, 0.5 m and 1.0 m, respectively. The results indicate that the largest tsunamis are expected on the Apulia and Gargano coasts of southern Italy. They found that focusing of energy due to bathymetric features enhances the tsunami heights.

At Stromboli volcano, southern Italy, on December 30, 2002, a moderate-sized landslide (with a volume of 0.02–0.03 km^3) generated a tsunami, with a maximum runup height of about 10 m. Because it occurred in the winter, there was no loss of human life,

nonetheless damage was caused on the coast. This slide occurred at Sciara del Fuoco (SdF), a steep scar of the island which can potentially produce a landslide with a volume of 1 km^3. TINTI *et al.* (2008) numerically simulated tsunamis from three other potential sources of landslides around the island. The expected landslide volume is similar to that of the 2002 slide. They showed that a landslide at Punta Lena, south of the island, can produce a tsunami even larger than the 2002 tsunami.

The paper by HEIDARZADEH *et al.* (2008) presented a deterministic assessment of tsunami hazard in the northwestern Indian Ocean by considering a series of six large (M_w 8.3) tsunamigenic earthquake scenarios along the Makran subduction zone. They used the tsunami model TUNAMI-2 (GOTO *et al.*, 1997), along with the GEBCO bathymetry grid, to calculate tsunami heights at the coastline for these scenarios. The calculated tsunami heights and arrival times were verified against observations of the tsunami caused by a Makran subduction zone earthquake that occurred in 1945. The scenario modeling demonstrated that earthquakes along the Makran subduction zone pose a substantial tsunami threat to the Arabian Sea coasts of Iran, Pakistan, Oman and India.

5. Probabilistic Tsunami Hazard Assessment

A further level of refinement in tsunami hazard assessment considers not only how large a tsunami affecting a particular community may be, but also how likely is the occurrence of a tsunami of a given magnitude. This is known as probabilistic tsunami hazard assessment, and its implementation is similar in concept to that of Probabilistic Seismic Hazard Assessment (CORNELL, 1968).

The paper by PARSONS and GEIST (2008) presents a probabilistic tsunami hazard assessment for the Caribbean region. This assessment involves consideration of both historical events, based on the impressive 500-year-long catalog of Caribbean tsunami observations, and also earthquake sources based on numerically-modelled seismic moment release along the convergent margins of the Caribbean plate. While the former potentially accounts for non-earthquake tsunami sources (e.g., submarine landslides), the latter accounts for earthquakes with long return periods that may not be represented in the catalog. The authors developed a Bayesian method for combining these to produce a tsunami hazard map that made optimal use of the information available from both the catalog and modeling results.

BURBIDGE *et al.* (2008) calculated probabilistic tsunami hazard for the coast of western Australia. Tsunamis from great earthquakes along the Sumbawa, Java and Sunda trenches have affected the western coasts of Australia. Probabilistic tsunami hazard was used to estimate offshore wave heights as a function of return period. While the tsunami heights along the Australian coasts from a magnitude 8 earthquake with the return period of about 100 years were not very high, those from a magnitude 9 earthquake, similar to the 2004 Sumatra-Andaman earthquake, with a return period of about 1,000 years, would be very large and potentially cause damage.

6. Tsunami Databases

Databases are essential for the support of tsunami hazard and risk assessments and warning systems. The task of collating information of varying quality from many different sources is a formidable one, and unless validated information about tsunami observations and observation platforms is made available in a consistent form, this information cannot be used effectively. Two papers in this issue discuss databases that are designed to provide effective support to hazard/risk assessment and warning systems.

MARRA *et al.* (2008) introduce readers to the concept of web services as a means to efficiently describe, collect, integrate, and publish sea-level station metadata that are contributed by many countries and organizations, and used by station operators, tsunami and other coastal hazard warning systems, disaster management officials, and coastal inundation researchers. The service incorporates an agreed-upon sea-level station XML schema for automatic and continuous station reporting, thus facilitating the implementation of always up-to-date data mining client applications. One example that is described is Tide Tool, which was developed by the Pacific Tsunami Warning Center to continuously download and decode sea-level data globally and to monitor tsunamis in real-time.

DUNBAR *et al.* (2008) describe the enhancements to the National Geophysical Data Center World Data Center for Geophysics and Marine Geology (WDC-GMG) national and international long-term tsunami data archive since 2004. The archive has expanded from the original global historical event databases and damage photo collection, to include tsunami deposits, coastal water-level data, DART buoy data, and high-resolution coastal Digital Elevation Model datasets for supporting model validation, guidance to warning centers, tsunami hazard assessment, and education of the public. The data are available in the public domain, and tools have been provided for interactive on-line and off-line data discovery and download in multiple formats to facilitate further integration and re-use by everyone.

Acknowledgments

Most of the papers included in this volume were presented in the tsunami session at the 2007 IUGG meeting held in Perugia, Italy. We thank all the participants who made that session such a success. We also thank the reviewers of each paper for their time and efforts, and Renata Dmowska and the editorial staff at Springer for their patience and support.

REFERENCES

BABA, T., MLECZKO, R., BURBIDGE, D., CUMMINS, P.R., and THIO, H. K. (2008), *The effect of the Great Barrier Reef on the propagation of the 2007 Solomon Islands tsunami recorded in northeastern Australia*, Pure Appl. Geophys. *165*, 2003-2018.

BURBIDGE, D., CUMMINS, P.R., MLECZKO, R., and THIO, H. K. (2008), *A Probabilistic Tsunami Hazard Assessment for Western Australia*, Pure Appl. Geophys. *165*, 2059–2088.

CORNELL, C.A. (1968), *Engineering seismic risk analysis*, Bull. Seismol Soc. Am. *58*, 1583–1606.

DIDENKULOVA, I., PELINOVSKY, E., and SOMERE, T. (2008), *Runup characteristics of symmetrical solitary tsunami waves of "unknown" shapes*, Pure Appl. Geophys., *165*, 2249–2264.

DUNBAR, P.K., STROKER, K.J., BROCKO, V.R., VARNER, J.D., MCLEAN, S.J., TAYLOR, L.A., EAKINS, B.W., CARIGNAN, K.S., and WARNKEN, R.R. (2008), *Long-term tsunami data archive supports tsunami forecast, warning, research, and mitigation*, Pure Appl. Geophys. *165*, 2275–2291.

FINE, I. V., CHERNIAWSKY, J. Y., RABINOVICH, A. B., and STEPHENSON, F. (2008), *Numerical modeling and observations of tsunami waves in Alberni Inlet and Barkley Sound, British Columbia*, Pure Appl. Geophys. *165*, 2019–2044.

GOTO, C., OGAWA, Y., SHUTO, N., and IMAMURA, F. (1997), *Numerical Method of Tsunami Simulation with the Leap-Frog Scheme (IUGG/IOC Time Project)*, IOC Manual, UNESCO, No. 35.

GREENSLADE, D.J.M. and TITOV, V. V. (2008), *Comparison study of two numerical tsunami forecasting systems*, Pure Appl. Geophys. *165*, 1991–2001.

HEIDARZADEH, M., PIROOZ, M.D., ZAKER, N.H., and SYNOLAKIS, C.E. (2008), *Evaluating tsunami hazard in the northwestern Indian Ocean*, Pure Appl. Geophys. *165*, 2045–2058.

MARRA, J., KARI, U.S., and WEINSTEIN, S.A. (2008), *A tsunami detection and warning-focused sea-level station metadata web service*, Pure Appl. Geophys. *165*, 2265–2273.

PARSONS, T. and GEIST, E.L. (2008), *Tsunami probability in the Caribbean region*, Pure Appl. Geophys., *165*, 2089–2116.

SYNOLAKIS, C., BERNARD, E.N., TITOV, V.V., KANOGLU, U., and GONZALEZ, F.I. (2008), *Validation and verification of tsunami numerical models*, Pure Appl. Geophys. *165*, 2197–2228.

TIBERTI, M. M., LORITO, S., BASILI, R., KASTELIC, V., PIATANESI, A., and VALENSISE, G. (2008), *Scenarios of earthquake-generated tsunamis for the Italian coast of the Adriatic Sea*, Pure Appl. Geophys. *165*, 2117–2142.

TINTI, S., ZANIBONI, F., PAGNONI, G., and MANUCCI, A. (2008), *Stromboli Island (Italy): Scenarios of tsunamis generated by submarine landslides*, Pure Appl. Geophys. *165*, 2143–2167.

TITOV, V.V. and GONZALEZ, F.I. (1997), *Implementation and testing of the Method of Splitting Tsunami (MOST) model*, NOAA Technical Memorandum ERL PMEL-112, 11 pp.

VILIBIĆ, I., MONSERRAT, S., RABINOVICH, A., and MIHANOVIĆ, H. (2008), *Numerical modelling of the destructive meteotsunami of 15 June 2006 on the coast of the Balearic Islands*, Pure Appl. Geophys. *165*, 2169–2195.

ZHANG, Y.J. and BATISTA, A. M. (2008), *An efficient and robust tsunami model on unstructured grids. Part I: Inundation benchmarks*, Pure Appl. Geophys. *165*, 2229–2247.

Pure appl. geophys. 165 (2008) 1991–2001
0033–4553/08/111991–11
DOI 10.1007/s00024-008-0413-x

Pure and Applied Geophysics

A Comparison Study of Two Numerical Tsunami Forecasting Systems

DIANA J. M. GREENSLADE[1] and VASILY V. TITOV[2]

Abstract—This paper presents a comparison of two tsunami forecasting systems: the NOAA/PMEL system (SIFT) and the Australian Bureau of Meteorology system (T1). Both of these systems are based on a tsunami scenario database and both use the same numerical model. However, there are some major differences in the way in which the scenarios are constructed and in the implementation of the systems. Two tsunami events are considered here: Tonga 2006 and Sumatra 2007. The results show that there are some differences in the distribution of maximum wave amplitude, particularly for the Tonga event, however both systems compare well to the available tsunameter observations. To assess differences in the forecasts for coastal amplitude predictions, the offshore forecast results from both systems were used as boundary conditions for a high-resolution model for Hilo, Hawaii. The minor differences seen between the two systems in deep water become considerably smaller at the tide gauge and both systems compare very well with the observations.

Key words: Tsunami, tsunami forecast.

1. Introduction

Recent tsunami events (e.g., Sumatra 2004, Java 2006, Solomon Islands 2007) have demonstrated the need for providing accurate and timely tsunami warnings for all the world's ocean basins. Improvements in the availability of sea-level observations and advances in numerical modelling techniques are increasing the potential for tsunami warnings to be based on numerical model forecasts. Numerical tsunami propagation and inundation models are well developed, but they present a challenge to run in real-time; partly due to computational limitations and also due to a lack of detailed knowledge on the earthquake rupture details (TITOV *et al.,* 2005). For these reasons, current tsunami forecast systems are based on pre-computed tsunami scenarios. A tsunami scenario is a single model run that is calculated ahead of time with the initial conditions carefully selected so that they are likely to represent an actual tsunamigenic earthquake.

This paper will present a comparison of two tsunami scenario databases: the NOAA/PMEL system (a.k.a. Short-term Inundation Forecast for Tsunamis – SIFT), currently

[1] Centre for Australian Weather and Climate Research, Bureau of Meteorology, GPO Box 1289, Melbourne, Victoria 3001, Australia. E-mail: d.greenslade@bom.gov.au

[2] NOAA Center for Tsunami Research, NOAA/PMEL/OERD, 7600 Sand Point Way NE, Bldg. 3, Seattle, WA 98115-0070, U.S.A.

being implemented at NOAA Tsunami Warning Centers and the Bureau of Meteorology system (T1), which has been developed for the Joint Australian Tsunami Warning Centre. Both scenario databases are based on the Method Of Splitting Tsunamis (MOST) model (TITOV and SYNOLAKIS, 1998), but there are some differences in the way the scenarios are constructed. These will be described in Section 2. A comparison of model forecasts for some recent events is presented in Section 3. The events chosen are the only two tsunamis that occur within the domains of both systems and for which a good set of deep ocean observations exists. Section 4 contains a discussion of the results.

2. *Description of the Scenario Databases*

2.1. T1 (Joint Australian Tsunami Warning Centre)

T1 is described in detail in GREENSLADE *et al.* (2007). It consists of a total of 741 scenarios calculated using the MOST model. The bathymetry data set used in the construction of the scenarios was extracted from a data set developed for the Bureau of Meteorology's ocean forecasting system (Mansbridge, unpublished document). The underlying bathymetry used in this data set is the Naval Research Laboratory Digital Bathymetry Data Base 2 arc minute resolution (NRL DBDB2). This has the GEBCO Digital Atlas merged into it south of 68°S, and the bathymetry used in the Australian region is the 2002 issue of Geoscience Australia's bathymetry and topography data set, with some manual adjustments incorporated. This merged 2 arc minute data set was sub-sampled at 4 arc minutes for T1.

The scenarios are distributed over 230 source locations in the Australian region. They are located 100 km apart along subduction zones (BIRD, 2003). Each source location has four scenarios associated with it, with magnitudes of 7.5, 8, 8.4 and 9. The defined rupture details for each scenario are listed in Table 1. Other details of the ruptures are fixed for each scenario. These are the depth (10 km), dip (25°) and rake (90°). TITOV *et al*. (1999) demonstrated that details of the first few tsunami waves are relatively insensitive to variations in the dip and the rake, so the impact of setting these parameters to be fixed for all scenarios is minimal. The current recommendation for using the scenarios operationally is that if the magnitude of an event is not one of the 4 magnitudes existing in the database, then the closest upper magnitude scenario should be used for forecast guidance. It is acknowledged that this could result in over-warning, which is a serious issue: The production of false alarms should be kept to a minimum within a tsunami warning system. However, over-warning is preferable to under-warning, which can result in direct catastrophic impacts. It should be noted that this "upper scenario" strategy is a temporary measure only and an enhanced scenario database with a scaling technique is currently being developed that will provide more appropriate guidance for intermediate magnitude earthquakes (SIMANJUNTAK and GREENSLADE, 2008).

Table 1

Rupture details for T1 scenarios

Magnitude (M_w)	*Width (W) (km)*	*Length (L) (km)*	*Slip (u_0) (m)*
7.5	50	100	1
8.0	65	200	2.2
8.4	80	400	3
9.0	100	1000	8.8

Specific details of the model configurations for the scenarios are: spatial resolution: 4 arc minutes, minimum offshore depth: 20 m, time step: 8 seconds, sea level (and depth-averaged currents) at every grid-point saved every 15 time steps (i.e., 2 minutes) and the model is run for 10 hours of model time.

2.2. *NOAA's Short-term Inundation Forecast (SIFT)*

The NOAA propagation database is described in detail in GICA *et al*. (2008). The forecast strategy is based on a unit source function methodology, whereby the model runs are individually scaled and combined to produce arbitrary tsunami scenarios. Each unit source function is equivalent to a tsunami generated by a M_w 7.5 earthquake with a rectangular fault 100 km by 50 km in size and 1 m slip. These are similar to the T1 M_w 7.5 events (see Table 1). The faults of the unit functions are placed adjacent to each other. When the functions are linearly combined, the resultant source function is equivalent to a tsunami generated by a combined fault rupture with assigned slip at each subfault.

The MOST model is used to generate the scenarios and the bathymetry for the Pacific Ocean is based on the SMITH and SANDWELL (1994) 2 arc minute data set. The model utilizes the bathymetry data in the original Mercator projection format of the Smith and Sandwell data, where the grid cells become smaller for locations farther away from the equator. The data are subsampled to twice coarser resolution (4 arc minutes at the equator) of the original dataset.

There are currently a total of 1400 unit sources distributed throughout the Pacific, Atlantic and Indian Oceans. These are arranged in several rows along known fault zones, to cover areas of potential tsunami sources. The rake is set at 90°, as in T1. The main differences with the T1 scenarios are that the dip and depth vary according to known assessments of the fault geometries (KIRBY *et al*., 2006). Where depth estimates are not available, the depth of the top row of sources is set at 5 km and the depth of the lower rows of sources depends on the dip of the top rows.

Other relevant specific details of the model configuration are: Spatial resolution: 4 arc minutes, minimum offshore depth: 20 m, time step: 15 seconds, sea level (and depth-averaged currents) at every fourth grid-point are saved every 4 time steps (i.e., 1 minute) and the model is run for 24 hours of model time.

For the model forecasts considered here, the NOAA system uses inversion techniques to select the best combination of unit source functions in order to match observations of sea level from the tsunameters (GICA *et al.*, 2008; TITOV *et al.*, 2005). The inversion is done by performing a positively-constrained combined least-squares fit of model-data comparisons for all DART locations for a given combination of unit sources. The inversion defines the scaling coefficients for each unit source in the combination.

3. Event Forecasts

Two different tsunami events are considered here. These particular events are chosen because they are in either the Indian or Southwest Pacific Oceans, and therefore occur within the domains of both systems (recall that the domain of T1 is limited to the Australian region). In addition, there are observations of sea level from deep-ocean buoys available for each event which can be used for inversion and/or verification. At the time of writing these were in fact the only events for which both these criteria were true, i.e., the events occurred within the domain of both systems and observations from deep-ocean buoys were available. With the current rapid expansion of the global tsunameter network, and the future expansion of the domain of T1, further tsunami events will provide more opportunities for comparison of the two forecasting systems.

3.1. Tonga 2006

The Tonga event occurred on May 3, 2006 at 15:26:39 (UTC) about 160 km northeast of Nuku'Alofa, Tonga. The first Pacific Tsunami Warning Center (PTWC) bulletin issued had the earthquake details as M_w 8.1 at (174.2°W, 19.9°S), with subsequent bulletins lowering the magnitude to 7.8. The United States Geological Survey (USGS) has analyzed the event as M_w 7.9 at 55-km depth and located at (174.164°W, 20.13°S). There were some minor impacts seen but no major injuries. Tide gauges in the region observed a tsunami with peak-to-trough wave heights of up to 50 cm.

The maps of maximum tsunami amplitude (H_{max}) from each system are shown in Figure 1. For the T1 database, this is the closest scenario to the actual event—in this case, the M_w 8.0 scenario with epicenter located at (173.4°W, 20.64°S). For the NOAA system, the best combination of unit sources to match the available tsunameter observations (see later) was a scaling factor of 6.6 applied to the time series of surface elevation associated with a single unit source located at (173.83°W, 20.43°S), which, in fact, is equivalent to a M_w 8.0 event. The distribution of H_{max} differs between the two systems predominantly because of the different source lengths: 200 km for T1 and 100 km for SIFT. The longer source results in a distribution of energy that is more focussed perpendicular to the fault

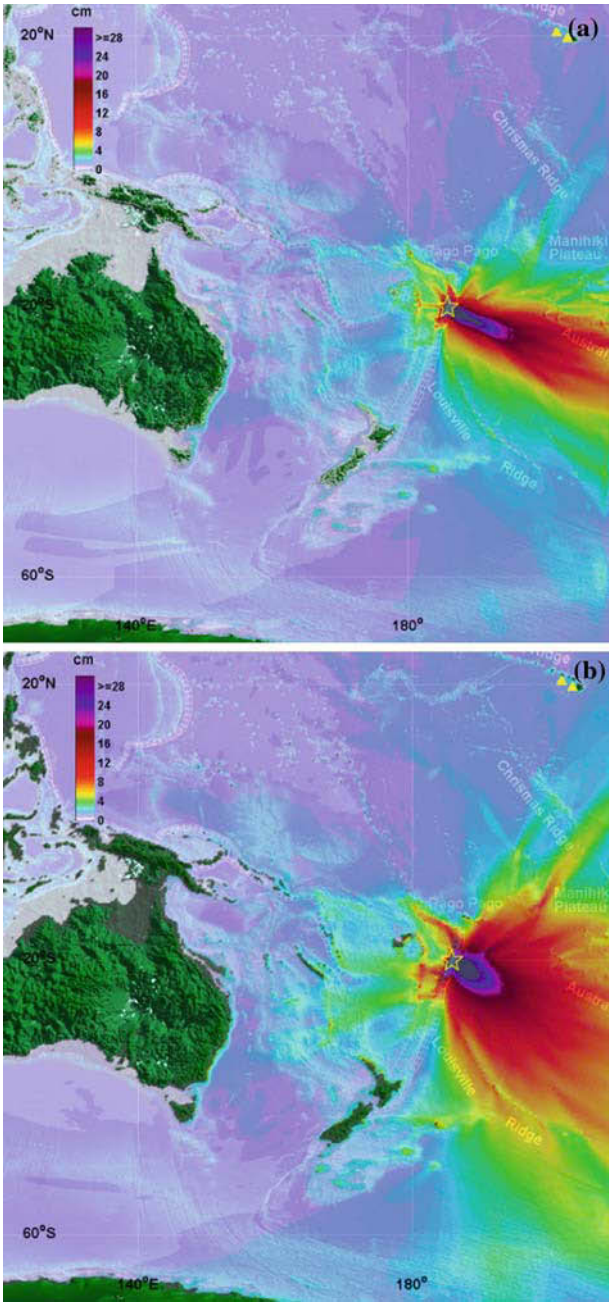

Figure 1
(a) Maximum tsunami amplitude from closest T1 scenario and (b) maximum tsunami amplitude from the SIFT system.

line while the shorter source acts more as a point source with energy distributed over a wider range of directions.

Observations of sea level in the deep ocean were available for this event from a Deep Ocean Assessment and Reporting of Tsunamis (DART) buoy (51407) at (203.493°E, 19.634°N) and an Easy-To-Deploy (ETD) DART buoy at (201.887°E, 20.5095°N) both near Hawaii. The locations of these buoys are shown by the yellow triangles in Figure 1. For each of the two systems, time series of sea level were extracted from the model output at the closest model grid point to the observation location. These time series are shown in Figure 2.

It can be seen that both systems compare well to the observations. For the DART (Fig. 2a), the time of arrival of the first crest from both systems matches the observed arrival time very well. In addition, the frequency of the wave appears very good, at least

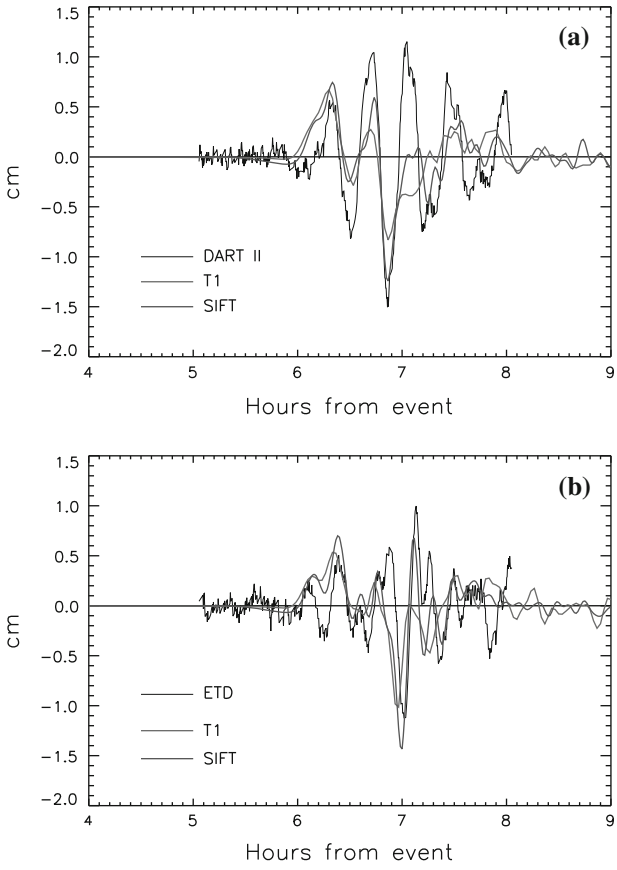

Figure 2
Time series of sea level elevation from tsunameters and scenario forecasts. (a) DART at (203.493°E, 19.634°N) and (b) ETD at (201.887°E, 20.5095°N) for the Tonga event.

for the first three waves. Both models miss the third crest and the overall decay in the amplitude of the waves from the models is more rapid than observed.

There are only minor differences between the two model time series—the SIFT results match the observed peak amplitudes slightly better—this is most likely a reflection of the fact that SIFT is scaled to match the observations, while the T1 result is raw model output that is not qualified by any data.

Comparisons at the ETD (Fig. 2b) are qualitatively similar. However, this time, the T1 scenario compares better in amplitude to a few of the peaks.

To investigate how the differences in the offshore forecasts would appear at the coast, a high-resolution model was run for Hilo, using both forecast results as boundary conditions. A high-resolution 2-D inundation simulation is run with the MOST model to obtain a local inundation forecast as part of the SIFT forecast procedures. The data input for the inundation computations is the result of the offshore forecast—tsunami parameters along the perimeter of the inundation computation area. The forecast inundation models (Stand-by Inundation Model—SIM) are optimized in order to obtain local forecasts in real time. Three levels of telescoping grids with increasing spatial resolution (down to 30 m for the finest grid) are employed to model local tsunami dynamics and inundation onto dry land. Each SIM is implemented and optimized for speed and accuracy, and validated thoroughly with historical tsunamis (TANG *et al.,* 2008). To date, over 30 SIMs have already been developed and are now available for forecasting.

The SIM for Hilo, Hawaii was used in this study to compare how differences between the two deep-water propagation forecasts manifest themselves at the tide gauge in Hilo harbor. Figure 3 shows that the small differences between the two scenarios observed in deep water have become even smaller for the tide gauge predictions. This, plus the good comparison with the observed gauge data, indicates that the nearshore dynamics of a tsunami may be only sensitive to the amplitude and period of the first few waves and is mostly driven by the local geometry of the harbor around the gauge. This is good news for database-driven forecast systems, since it suggests that uncertainties in the model tsunami source definition may not be crucial for accurate coastal forecasts, provided that the amplitude and period of the approaching tsunami are captured correctly. More comparisons at different coastal locations relative to the source may show alternate differences between the methods. While this test at an individual location cannot be conclusive, the results are encouraging, showing, at least, that small differences offshore, result in small (or even smaller) differences at the coast.

3.2. Sumatra 2007

On September 12, 2007 at 11:10:26 (UTC) an earthquake occurred off southern Sumatra. This event had some significant impacts with 25 fatalities and numerous people injured. PTWC's initial Tsunami Bulletin had the magnitude of the earthquake set at M_w

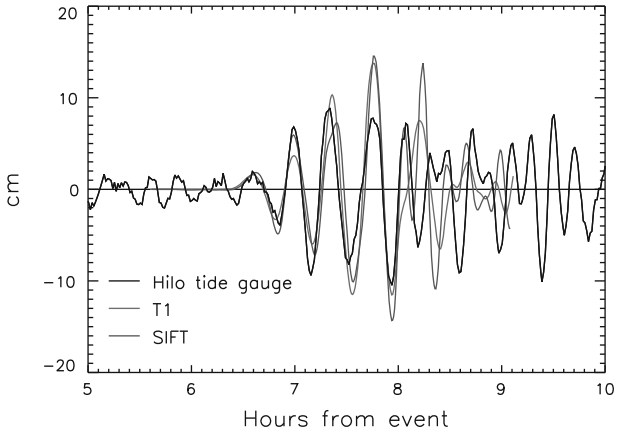

Figure 3
Time series of surface elevation at the Hilo tide gauge and from the inundation model fed by the two scenario databases.

7.9. This was subsequently raised to M_w 8.2 for the second and all subsequent bulletins. USGS has analyzed the event to be M_w 8.4 at (101.374°E, 4.520°S) and depth 55 km. The event was recorded at DART buoy 23401, to the west-northwest of Phuket at (88.54°E, 8.9°N) (see Fig. 4). A tsunami wave of 2 cm amplitude was observed by the instrument.

For the T1 database, the closest scenario to the event is the M_w 8.4 scenario with epicenter located at (100.53°E, 4.9°S). The distribution of H_{max} from T1 is shown in Figure 4. Data recorded by the DART and transmitted in real time were used to constrain the SIFT propagation forecast for the associated tsunami via a process of selecting the combination of unit sources that provided the best fit to the observed signal at the DART. The DART-inverted source used three database segments with scaling factors of 8.7, 5.6 and 3.9 on the three unit fault segments which correspond to an M_w 8.3 model tsunami source (Fig. 4).

The time series of surface elevation from the two databases at the location of the DART is shown in Figure 5. Both systems capture the arrival time of the tsunami at the DART very well. The SIFT database marginally overestimates the first peak, while the T1 forecast of the peak is too broad. SIFT also captures the first trough very well, while the T1 forecast misses it. Both systems miss the second peak but fit the third peak quite well, with T1 being slightly closer in amplitude.

At the time of the tsunami, the SIFT database for the Indian Ocean had not been completed and only the two shallowest rows of unit sources had been precomputed. This event might therefore be better described with additional deeper fault segments. Despite this potential limitation, the comparison of the modelled SIFT time series with observations at the DART shows a fairly good fit.

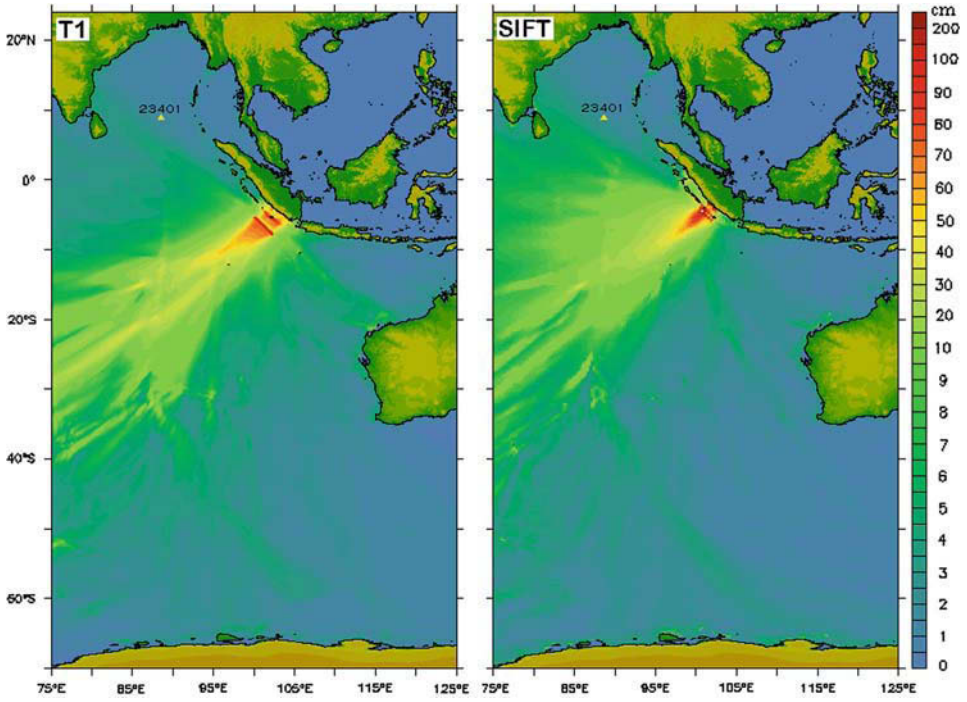

Figure 4
Maximum computed offshore amplitudes for the September 12, 2007 Sumatra tsunami from T1 (left panel) and SIFT (right panel).

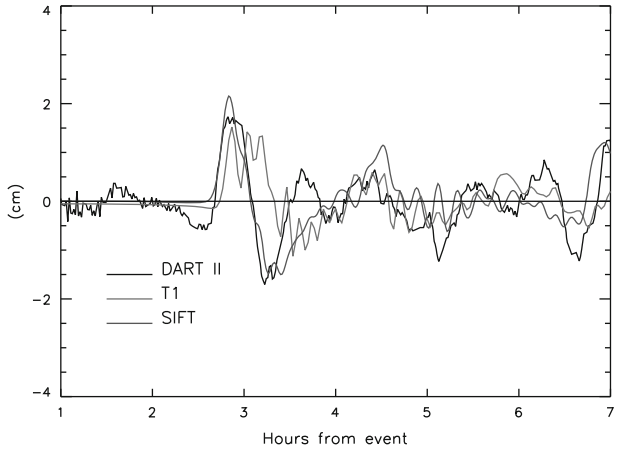

Figure 5
Time series of sea level elevation from scenario forecasts for the Sumatra event compared to the DART.

4. Discussion

The two forecast systems considered in this study employ a similar modelling strategy that is based on a precomputed database of propagation runs. Use of the same model and a similar database structure allows for potential interconnection between the two databases in many different ways. Each system can potentially use the other system's scenarios for an event assessment to complement, double-check or extend forecasts to larger or different regions.

This comparison study is the first attempt to investigate potential similarities, differences, benefits and limitations of two forecast systems.

The obvious advantage of the T1 approach is the simplicity and speed of use, which may lead to fast and robust forecast procedures. The individual precomputed scenarios can be linked to precomputed warning structures which can then be rapidly disseminated (ALLEN and GREENSLADE, 2008). In fact, once the magnitude of the earthquake is known, the relevant warnings can be produced almost instantaneously. Considering that the T1 forecasts are "blind runs" and completely independent of the tsunameter data, the system compares very well to the observations. The SIFT method assimilates real-time tsunami measurements into the forecast, in addition to seismic estimates. The method comes with the price of a complex data inversion process and multi-step forecast procedure. While the seismic-based forecast can be obtained as soon as the magnitude is known, the final SIFT forecast is based on real-time tsunami measurements and can be done only after receiving data from tsunameters. The SIFT method is more flexible, can potentially reproduce complex tsunami sources and provide high accuracy. It also includes high-resolution coastal forecasts to reproduce coastal dynamics.

The different implementations of the model tsunami sources lead to differences in the forecast results. However, the differences in the offshore forecasts are surprisingly small, at least where validation observations were available. The test comparison of the coastal forecast at one location (Hilo) showed even smaller differences for the Tonga event. These results are encouraging, since they demonstrate consistency in the forecast results. This is important for establishing a common ground for warning procedures for this inherently international phenomenon that requires an international response.

Acknowledgements

The authors would like to thank Liujuan (Rachel) Tang, Mick Spillane, Stewart Allen and Arthur Simanjuntak for valuable contributions to the manuscript. This publication is partially funded by the Joint Institute for the Study of the Atmosphere and Ocean (JISAO) under NOAA Cooperative Agreement No. NA17RJ1232, Contribution #1589.

REFERENCES

ALLEN, S.C.R. and GREENSLADE, D.J.M. (2008), *Developing Tsunami warnings from numerical model output*, Nat. Hazards, doi:10.1007/s11069-007-9180-8.

BIRD, P. (2003), *An updated digital model of plate boundaries*, Geochem. Geophys. Geosys. *4*(3), 1027, doi:10.1029/2001GC000252.

GICA, E., SPILLANE, M.C., TITOV, V.V., CHAMBERLIN, C.D., and NEWMAN, J.C. (2008), *Development of the forecast propagation database for NOAA's Short-Term Inundation Forecast for Tsunamis (SIFT)*, NOAA Tech. Memo. OAR PMEL-139, 89 pp.

GREENSLADE, D.J.M, SIMANJUNTAK, M.A., CHITTLEBOROUGH, J., and BURBIDGE, D. (2007), *A first-generation real-time tsunami forecasting system for the Australian region*, BMRC Research Report No. 126, Bur. Met., Australia.

KIRBY, S., GEIST, E.L., LEE, W.H.K., SCHOLL, D., and BLAKELY, R. (2006), *Tsunami source characterization for western Pacific subduction zones: A preliminary report*, Tsunami Sources Workshop, 2006, http://walrus.wr.usgs.gov/tsunami/workshop/.

MANSBRIDGE, J., *Bathymetry comparisons*, unpublished document, CSIRO.

SIMANJUNTAK, M.A. and GREENSLADE, D.J.M. (2008), *Towards a scaling method for a tsunami scenario database: The effect of wave dispersion*, EGU General Assembly 2008, Vienna, Austria.

SMITH, W.H.F. and SANDWELL, D.T. (1994), *Bathymetric prediction from dense satellite altimetry and sparse shipboard bathymetry*, J. Geophys. Res. *99*, 21,803–21,824.

TANG, L., TITOV, V.V., WEI, Y., MOFJELD, H.O., SPILLANE, M., ARCAS, D., CHAMBERLIN, C., BERNARD, E.N., GICA, E., and NEWMAN, J. (2008), *Tsunami Forecast Analysis for the May 2006 Tonga Tsunami*, J. Geophys. Res., accepted.

TITOV, V.V., MOFJELD, H.O., GONZALEZ, F.I., and NEWMAN, J.C. (1999), *Offshore forecasting of Alaska-Aleutian Subduction Zone tsunamis in Hawaii*, NOAA Technical Memorandum ERL PMEL-114, 22 pp.

TITOV, V.V., GONZÁLEZ, F.I., BERNARD, E.N., EBLE, M.C., MOFJELD, H.O., NEWMAN, J.C., and VENTURATO, A.J. (2005), *Real-time tsunami forecasting: Challenges and solutions*, Nat. Hazards *35*(1), 41–58.

TITOV, V.V. and SYNOLAKIS, C.E. (1998), *Numerical Modeling of Tidal Wave Runup*, J. Waterw. Port Coast. Ocean Eng. *124*(4), 157–171.

(Received January 17, 2008, revised June 3, 2008)

Pure appl. geophys. 165 (2008) 2003–2018
0033–4553/08/112003–16
DOI 10.1007/s00024-008-0418-5

Pure and Applied Geophysics

The Effect of the Great Barrier Reef on the Propagation of the 2007 Solomon Islands Tsunami Recorded in Northeastern Australia

Toshitaka Baba,[1,2] Richard Mleczko,[2] David Burbidge,[2] Phil R. Cummins,[2] and Hong Kie Thio[3]

Abstract—The effect of offshore coral reefs on the impact from a tsunami remains controversial. For example, field surveys after the 2004 Indian Ocean tsunami indicate that the energy of the tsunami was reduced by natural coral reef barriers in Sri Lanka, but there was no indication that coral reefs off Banda Aceh, Indonesia had any effect on the tsunami. In this paper, we investigate whether the Great Barrier Reef (GBR) offshore Queensland, Australia, may have weakened the tsunami impact from the 2007 Solomon Islands earthquake. The fault slip distribution of the 2007 Solomon Islands earthquake was firstly obtained by teleseismic inversion. The tsunami was then propagated to shallow water just offshore the coast by solving the linear shallow water equations using a staggered grid finite-difference method. We used a relatively high resolution (approximately 250 m) bathymetric grid for the region just off the coast containing the reef. The tsunami waveforms recorded at tide gauge stations along the Australian coast were then compared to the results from the tsunami simulation when using both the realistic 250 m resolution bathymetry and with two grids having fictitious bathymetry: One in which the the GBR has been replaced by a smooth interpolation from depths outside the GBR to the coast (the "No GBR" grid), and one in which the GBR has been replaced by a flat plane at a depth equal to the mean water depth of the GBR (the "Average GBR" grid). From the comparison between the synthetic waveforms both with and without the Great Barrier Reef, we found that the Great Barrier Reef significantly weakened the tsunami impact. According to our model, the coral reefs delayed the tsunami arrival time by 5–10 minutes, decreased the amplitude of the first tsunami pulse to half or less, and lengthened the period of the tsunami.

Key words: Tsunami, the Great Barrier Reef, the 2007 Solomon Islands earthquake.

1. Introduction

The coral reefs offshore Sri Lanka reportedly reduced the impact of the 2004 Indian Ocean tsunami (Fernando *et al.*, 2005). Where there were gaps in the reef the tsunami was able to inundate up to 1.5 km inland. Yet, a few kilometers away where coral reefs

[1] Department of Oceanfloor Network System Development for Earthquakes and Tsunamis, Japan Agency for Marine - Earth Science and Technology, 2–15 Natsushima - cho, Yokosuka-city, Kanazawa 2370061, Japan. E-mail: babat@jamstec.go.jp

[2] Geoscience Australia, GPO Box 378, Canberra ACT 2601, Australia.

[3] URS Group Inc., 556 El Dorado Street, Pasadena, California 91101, U.S.A.

did not have gaps, the wave only travelled 50 m inland. A numerical study indicated that the healthy reefs off the coast produced at least twice as much protection as dead reefs by using an idealized model of tsunami impact on a reef-bounded shoreline (KUNKEL *et al*., 2006). By contrast, in Banda Aceh, Indonesia, the presence or absence and condition of coral reefs made no difference in the impact of the giant Indian Ocean tsunami that penetrated kilometers inland (ADGER *et al*., 2005; BAIRD *et al*., 2005). To our knowledge, there has been no quantitative comparison between observed and calculated wave runup heights or inundation distance due to the presence or absence of reefs for this region. This is probably due to lack of publicly available, accurate bathymetric data which is essential for accurate numerical simulation of a tsunami. Accordingly, more work is needed to confidently conclude that coral reefs can mitigate tsunami damage along the coast.

A great earthquake occurred on 1 April, 2007 at the southern New Britain-San Cristobal trench off the Solomon Islands (the 2007 Solomon Islands earthquake). This earthquake ruptured the plate boundary of the Pacific plate with, respectively, the Australia, Woodlark, and the Solomon Sea plates. The magnitude of the earthquake was estimated to be 8.1 by the U.S. Geological Survey (USGS). Because it was a large submarine earthquake, it generated a large tsunami which left 52 people dead and more than 7,000 people homeless in the Solomon Islands. The tsunami also propagated into the Coral Sea and reached the Australian coast over the Great Barrier Reef (GBR), the world's largest coral reef system. The Great Barrier Reef was approximately 1,500 km from the source of the tsunami. Clear (but small) tsunami waveforms were recorded by tide gauges in northeastern Australia at communities behind the Great Barrier Reef. Geoscience Australia's 250 m gridded bathymetric dataset (GA250, see Fig. 1) was fortunately available to calculate the tsunami from this event. This dataset was compiled from 20 years accumulation of bathymetric survey data acquired by various organisations in the waters offshore Australia.. We believe that the data density is generally sufficient to represent the configuration of the coral reefs in the numerical simulation reasonably well, although there are noticeable gaps in parts of the data coverage. The tsunami observation and bathymetric dataset, therefore, provided a good opportunity to model the effect of the GBR on tsunami propagation.

We investigate the 2007 Solomon Islands tsunami in this paper. Since the tsunami was caused by the sea-floor deformation due to an underwater earthquake, initially an earthquake rupture model is required. We calculate this by inverting the teleseismic waves observed worldwide from this event. This is then used to calculate the initial sea-floor deformation based on a linear elastic dislocation model. Propagation of the 2007 Solomon Islands tsunami is modelled by solving the linear shallow water equations using the GA250 bathymetry dataset for the region near the coast. Furthermore, two tsunami simulations are performed in which the GBR in GA250 is replaced with fictitious bathymetry for purposes of comparison. We focus here on the bathymetric effects of the GBR on the tsunami propagation rather than other potential effects on the wave such as its sensitivity to the earthquake rupture model.

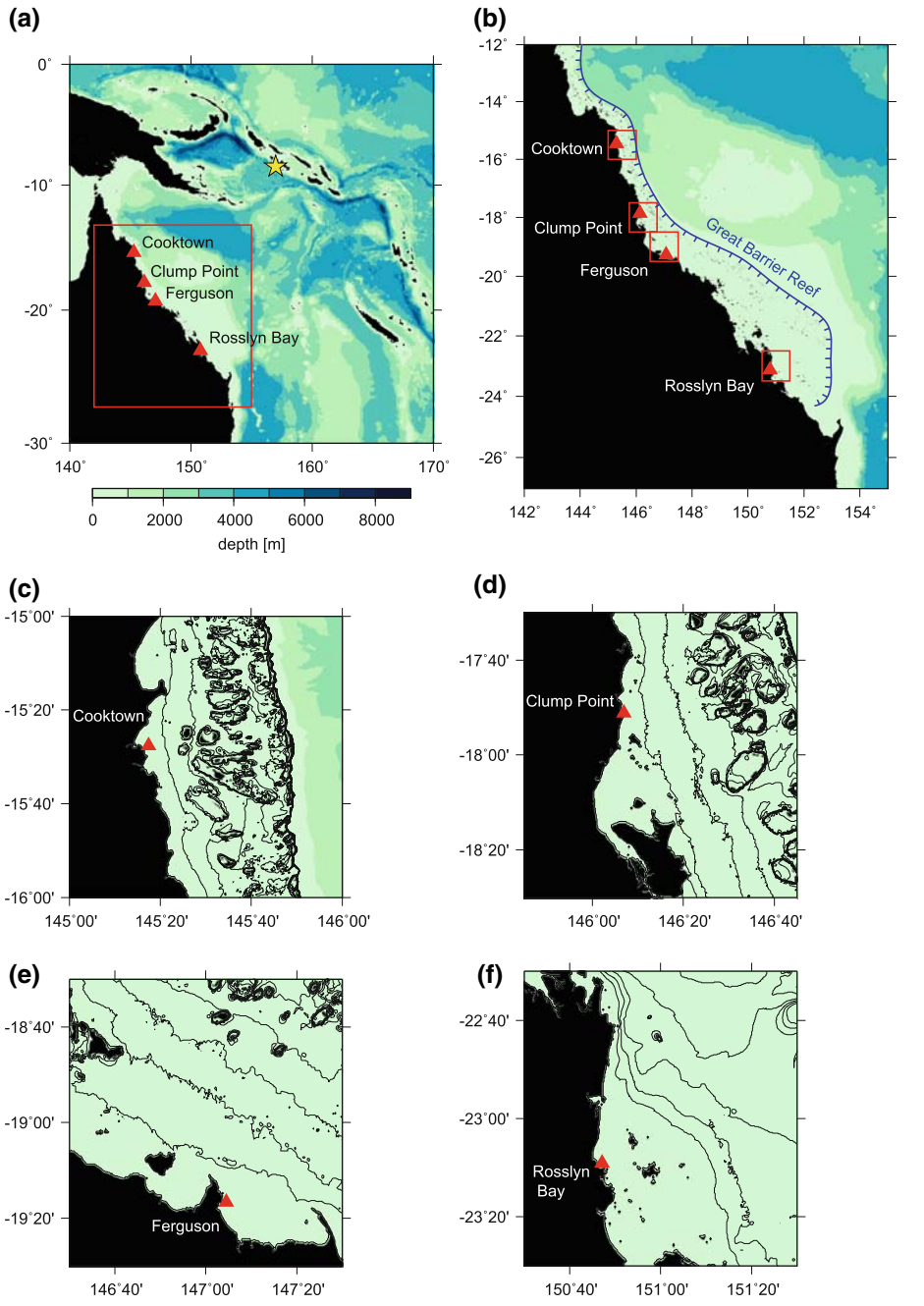

Figure 1

Bathymetric maps for: (a) the entire computational domain (90” grid spacing, a combination of the GA250 and DBDB2 bathymetry grids)), (b) GBR area (30” grid spacing) and (c-f) areas near tide gauges (10” grid spacing), both based on the GA250 bathymetry grid. Red squares show the areas of finer bathymetry used in the tsunami computation. Star and triangles indicate the epicenter of the 2007 Solomon Islands earthquake and tide gauges, respectively.

2. Initial Sea-Surface Deformation of the 2007 Solomon Islands Tsunami

To estimate the rupture model of the 2007 Solomon Islands earthquake, we applied the multiple time window method described in THIO *et al.* (2004). GSN (Global Seismological Network) data were downloaded from the IRIS DMC (http://www.iris.washington.edu/). We selected 19 teleseismic P and 17 SH waveforms based on the quality of the data and the station distribution (Fig. 2a). The waveforms were then converted to displacement and bandpass-filtered between 4 mHz and 4 Hz. The first 100 seconds after the arrival times of P and S waves were included in the inversion. Rayleigh and Love waves recorded at 21 sites were also used in order to stabilize the inversion. These surface waves were bandpassed-filtered between 3 mHz and 6 mHz.

The strike of the fault plane used in the inversion was adjusted from the approximately 330° azimuth obtained in the Global (formerly Harvard) CMT inversion to 307°, so as to better match the strike of the trench as expressed by water depth contours in this area. We experimented with a range of fault-dip angles between 10° and 50° and found that a dip angle of 35° produces the smallest misfit between the observed and synthetic SH waves (Fig. 3). This dip angle was consistent with the fault mechanism of this event obtained by the Global CMT Project and with the subduction angle of the plate shown by marine seismic surveys of this area (MIURA *et al.*, 2004; YONESHIMA *et al.*, 2005). The rake angle was determined from the inversion but was constrained to be $90° \pm 45°$. The total maximum dimensions of the fault plane were assumed to be 300 km × 100 km. This was divided into 20 km × 20 km subfaults and the slip and rake was determined for each subfault. The hypocenter location determined by the USGS was used as the rupture starting point, that is latitude −8.481°, longitude 156.978°, and depth 10.0 km.

Figure 2b shows the cumulative slip distribution of the 2007 Solomon Islands earthquake obtained by the seismic inversion. The earthquake rupture propagated unilaterally along the strike direction to the northwest. The dimension of the area of significant fault slip was about 180 km × 80 km. There was a large slip patch about 140 km to the northwest of the hypocenter and a moderate slip patch near the hypocenter. The maximum amount of slip was estimated to be about 5.2 m. The estimated moment magnitude was 8.1, consistent with the NEIC and the Global CMT solutions. The variance reduction (VR) of the seismic waveforms (determined by $1-\Sigma(d_{obs}-d_{cal})^2/\Sigma d_{obs}^2$) was 66%, where d_{obs} and d_{cal} indicate normalized observed and calculated waveforms, respectively. Figure 4 shows the calculated and observed seismic waves used in the inversion.

The vertical deformation at the seafloor was calculated using the equations of OKADA (1992) for a dislocation in an elastic half-space, and the seafloor deformation we obtained is shown in Figure 2c. A Poisson's ratio of 0.25 was used in the calculation. Most of the area over the earthquake source region was uplifted and all the area of significant uplift (over 1 m of uplift) was beneath the sea. Thus this event would be very effective in generating a tsunami. The maximum amount of uplift was about 2.1 m. We assumed that the seafloor deformation was the same as the initial wave height of the tsunami.

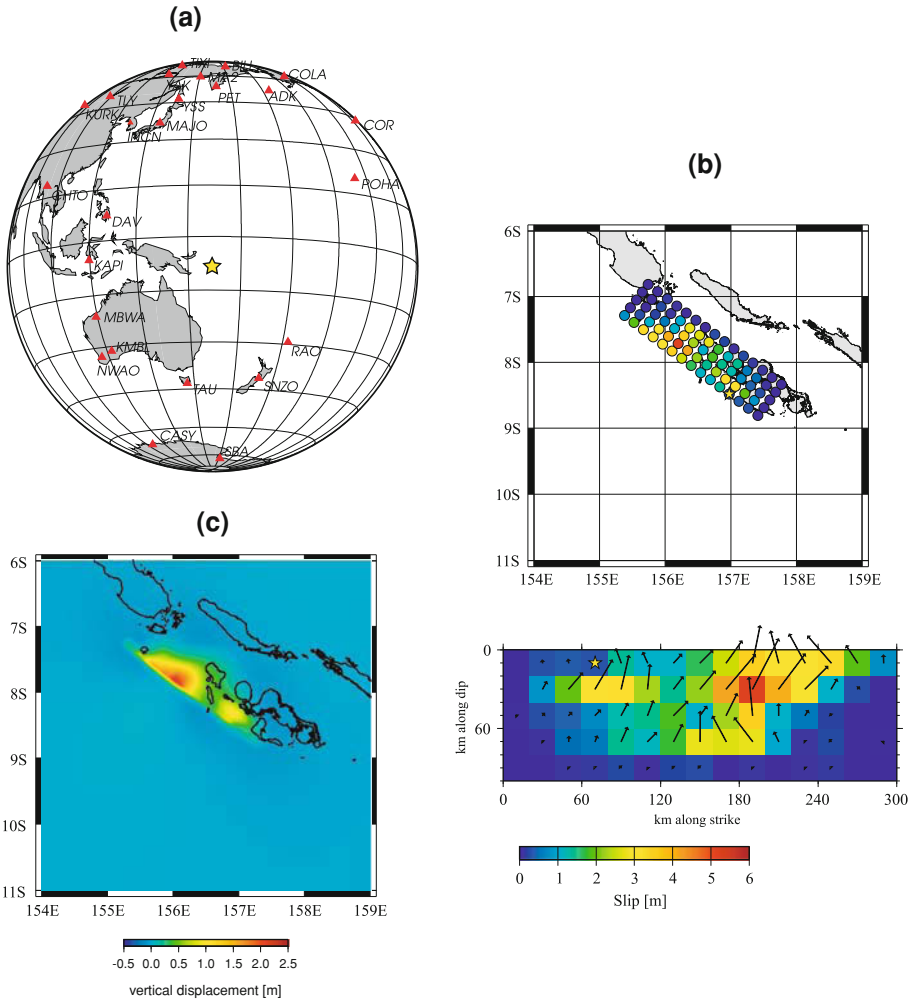

Figure 2
(a) Seismic station distribution (triangles) used in the inversion. Star shows the epicenter of the 2007 Solomon Islands earthquake. (b) Cumulative slip distribution on the fault plane during the event. The color shows the slip amount and arrows represent the motion of the hanging wall relative to the footwall. The star shows the rupture starting point (hypocenter). (c) Coseismic seafloor vertical displacements derived from the obtained slip distribution.

3. *Numerical Simulation of the 2007 Solomon Islands Tsunami*

The 2007 Solomon Islands tsunami, after passing over the GBR, was observed by the network of storm tide gauges operated by the Environment Protection Agency of Queensland, Australia. The storm tide network was adjusted so as to record changes in water-levels each minute immediately after the earthquake. Normally, these gauges record water-level changes every 10 minutes, however, this sampling period would not

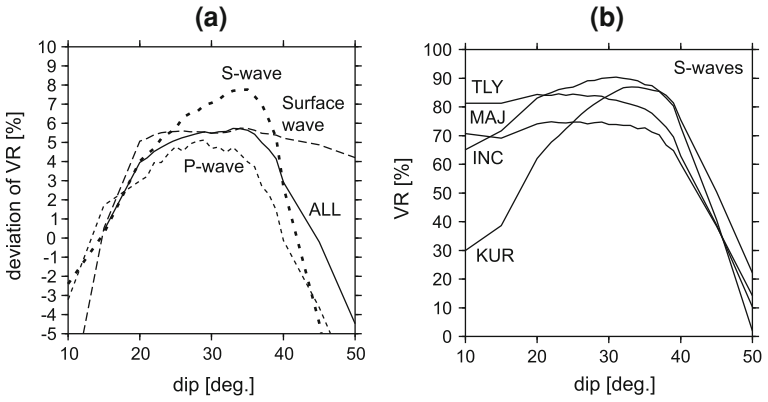

Figure 3

(a) Variance reductions as a function of fault-dip angle calculated for observed vs. synthetic P, S, surface wave, and a combination of all of these. The curves are deviations from the value obtained from assuming a dip angle of 15 degrees. A clear peak was found around a dip angle of 35 degrees by the S-wave curve. (b) Variance reductions as a function of dip for S-waves recorded at TLY, MAJ, INC and KUR (see Fig. 2a).

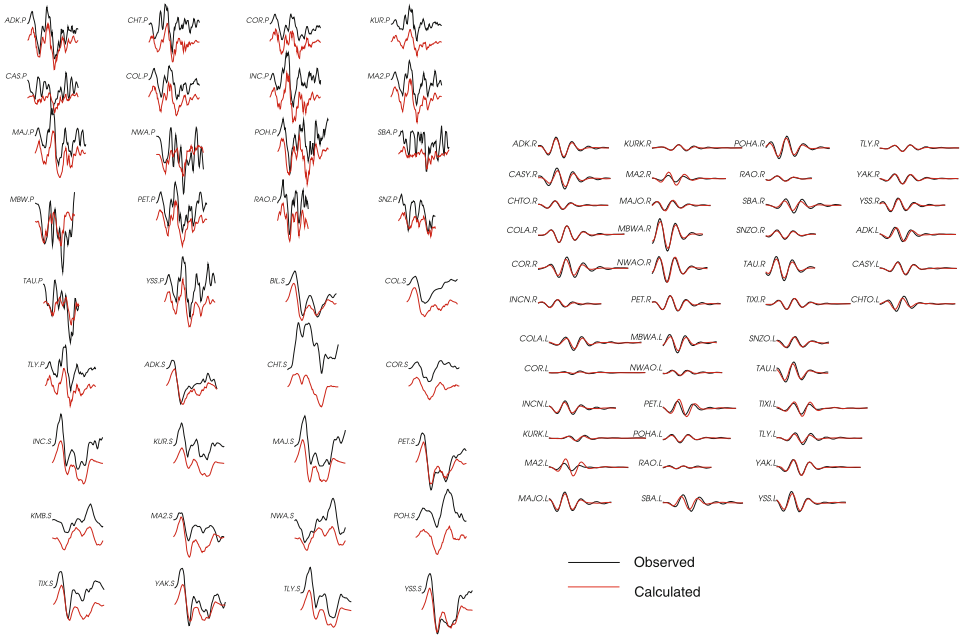

Figure 4

Comparison between the calculated (black) and observed teleseismic waveforms (red) of the 2007 Solomon Islands earthquake. Station names and components (P: vertical component P wave, S: SH wave, R: Rayleigh wave, L: Love wave) are shown. Zero level of the calculated body waves was shifted downward for ease of comparison.

have provided sufficient resolution to accurately detect the tsunami event. They provided 21 tsunami waveforms recorded by the network in a report (ENVIRONMENT PROTECTION AGENCY, 2007). While most tide gauges recorded a tsunami wave height in crest to trough of less than 0.3 m, the gauges at Clump Point and Rosslyn Bay both recorded a wave of about 0.5 m crest to trough. We used the data recorded at the 4 stations shown in Figure 1, based on quality and station distribution.

In the present study, the propagation of the 2007 Solomon Islands tsunami was modelled by solving the equations of linear shallow-water wave theory. We used the method of ICHINOSE *et al*. (2007) which was modified from the uniform finite-difference scheme described in SATAKE (2002) to include a variable nested grid scheme. Three grids were used in the tsunami computation. The coarsest grid was used to represent the entire computational domain, including the tsunami source and the tide gauge stations, stretching from 140°E to 170°E and 30°S to 0°S (Fig. 1a). The bathymetry used for this grid was defined using a combination of GA250 in that part of the computational domain that it covers, i.e., south of 10°S and west of 155°E, and the global bathymetry grid DBDB2 for the rest of the domain. DBDB2 is a global 2 arc-minute bathymetry grid assembled by the U.S. Naval Research Laboratory (www7320.nrlssc.navy.mil/DBDB2_WWW). These bathymetry grids were subsampled and interpolated, respectively, to 90 arc-sec spacing. Nested within this coarse grid is a medium-resolution grid of 30 arc-second spacing defined over the area indicated in Figure 1b by subsampling GA250. Finally, nested within the medium-resolution grid is a series of high-resolution grids covering the areas near the tide gauges indicated in Figures 1c–1f, whose 10 arc-second spacing is almost equal with the original grid spacing of GA250 (250 m). It is important to note that points of the high-resolution grid near the Australian coast that had a water depth less than 10 m were reset to be exactly 10 m deep (i.e., no point had a depth between 0 and 10 m). This helped to ensure the stability and validity of our numerical model, which uses the linear shallow water wave equations to calculate the tsunami waveforms. The linear shallow water equations assume that the wave amplitude is much smaller than the water depth, which may not be true in shallow waters (less than 10 m). The rise time of the initial wave height was assumed to be 60 seconds, based on the source duration of the 2007 Solomon Islands earthquake. The time step used in the computation was 0.5 seconds in order to satisfy the stability condition of the finite-difference calculation in the finest grid.

Figure 5 shows comparisons between the observed and the computed tsunami waveforms derived from the teleseismic source model of the 2007 Solomon Islands earthquake. In the previous report by the Environment Protection Agency (2007), the numerical simulation of the Solomon Islands tsunami did not match the observations well. Arrival times of the tsunami wave were noticeably later by about 30 minutes than those they had predicted. Our model indicated misfits of arrival time less than 5 minutes at Cooktown, Clump Point and Ferguson and about 10 minutes at Rosslyn Bay. This improvement was a consequence of the use of good bathymetric data near the coastline and the GBR. However, the computed wave heights were still slightly smaller than the observations.